International Journal of Thermophysics, Vol. 28, No. 3, June 2007 (© 2007)
DOI: 10.1007/s10765-007-0191-1

About the Proper Wavelength for Pyrometry on Shock Physics Experiments

Achim Seifter[1,2] **and Andrew W. Obst**[1]

Usually one wants to measure the thermal radiance emitted by a hot-surface at a wavelength as short as possible, since the uncertainty in the true temperature due to unknown emissivity decreases with decreasing wavelength. Unfortunately the radiance also decreases with decreasing wavelength, and hence the signal-to-noise ratio becomes worse with shorter wavelengths. Depending on what temperature range is to be covered, a reasonable compromise can be found for most applications. When pyrometry is applied to shock physics experiments, there is an additional factor that has to be taken into consideration. Due to the nature of shock physics experiments, one has to deal with background light caused by flashes from air lighting up, high-explosive light, and muzzle flash from a powder gun, etc. In addition, even if the experiment is designed appropriately, there is often a temperature non-uniformity as well as thermal radiation from transparent anvils that are used to increase the interface pressure. In most cases, there is no engineering approach to minimize these temperature non-uniformities. The sensitivity to these non-uniformities increases with decreasing wavelength for the very same reason that the sensitivity to uncertainties in emissivity is increasing. This paper describes the above problems, deals with the problem of temperature non-uniformity in detail, and presents arguments why single-wavelength pyrometry in shock physics experiments can be very deceiving even in well designed experiments.

KEY WORDS: blackbody radiation; infrared; pyrometry; shock physics.

[1] Los Alamos National Laboratory, Physics Division, MS E526, Los Alamos, New Mexico, 87545, U.S.A.
[2] To whom correspondence should be addressed. E-mail: seif@lanl.gov

0195-928X/07/0600-0934/0 © 2007 Springer Science+Business Media, LLC

1. INTRODUCTION

1.1. Pyrometry Basics

The thermally emitted radiation of a hot-surface at a given wavelength and temperature is the product of the spectral intensity of a blackbody and the normal spectral emissivity at this temperature and wavelength.

$$L(T,\lambda) = \frac{c_1}{\lambda^5\left(e^{\frac{c_2}{\lambda T}} - 1\right)}\varepsilon(T,\lambda) \tag{1}$$

where $L(T, \lambda)$ is the thermal radiation of a surface at temperature T at wavelength λ within the wavelength interval $d\lambda$ into the solid angle $d\Omega$, c_1 and c_2 are the first and second Planck radiation constants, and ε is the normal spectral emissivity.

Figure 1 shows the ratio of the normal spectral radiance of a blackbody and the wavelength to the 5th power as well as the ratio of the relative change of radiance and the relative change of temperature as a function of the product of wavelength and temperature. The maximum of the thermal radiance occurs at a wavelength $\lambda_{\max} = 2897.7(\mu\mathrm{m}\cdot K)/T$. This relation is known as Wien's displacement law.

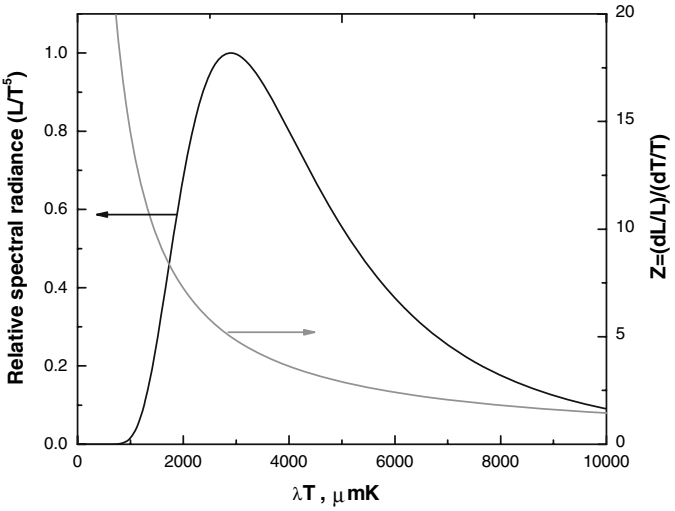

Fig. 1. Relative thermal radiation as well as ratio of change in radiance and relative change in temperature as a function of the product λT.

The normal spectral emissivity for a smooth surface can be calculated from the optical properties (complex index of refraction) of the material. The contribution of surface roughness to the normal spectral emissivity is not totally understood and can only be modeled for simple cases [1, 2]. This complicates the situation for shock physics experiments dramatically, because even if one starts with a smooth surface, this condition changes immediately after breakout of the shock wave at the surface under investigation. Since *in situ* measurements of the normal spectral emissivity in shock physics experiments are very difficult, one has to estimate its value. The uncertainty in the emissivity manifests itself directly as an uncertainty in the thermal radiance (see Eq. (1)) and hence as an uncertainty in the calculated true temperature. Since the relative change in radiance divided by the relative change in temperature increases with decreasing wavelength (see Fig. 1), one can minimize the uncertainty in temperature by determining the thermal radiance at a wavelength as short as possible: $((\Delta T/T) = (1/Z)(\Delta L/L) = (1/Z)(\Delta\varepsilon/\varepsilon))$[3] .

1.2. Additional Problems with Pyrometry when Applied to Shock Physics

In most applications of pyrometry, the arguments mentioned above (combined with a knowledge of photon detectors, optics, fibers, and the temperature range to be covered) are sufficient to decide on a reasonable wavelength for a pyrometer [4]. In shock physics the situation is more complicated because of an additional set of problems inherent to these kinds of experiments. The most important of these complications are:

- Light from high explosives or laser light getting into the optical path of the pyrometer.
- Lighting up of air in front of the surface of interest due to the high dynamic pressure (nitrogen luminescence).
- Hot-spots on the surface under investigation due to surface roughness, porosity, inhomogeneities in the sample composition, shear-banding, ejecta, and microjets.
- Thermal radiation of a transparent anvil (LiF or Al_2O_3 crystals in many cases) attached to the surface in order to enhance the interface pressure.

While the problems mentioned in the first two bullets can be avoided in most cases by a proper design of the experimental hardware [4–6], the problems mentioned in the latter two bullets can only be minimized (if at all)

[3] Since the thermal radiance decreases with decreasing wavelength, the signal-to-noise ratio decreases as well, while the noise equivalent temperature [3] increases. The combined uncertainty due to unknown emissivity and noise in the signal should be a minimum at the proper wavelength of the pyrometer.

and have to be addressed by the way the pyrometer is designed and the obtained data are analyzed.

1.3. Multiwavelength Approaches

If a measurement of the normal spectral emissivity cannot be done simultaneously with the thermal radiation measurement, then one can either estimate an emissivity value or apply one of the many multiwavelength approaches described in the literature [7]. The basic idea of these approaches is that although the absolute value of the emissivity is not known, there is some knowledge of its spectral behavior. If the thermal radiance, for example, is measured at two wavelengths, then one can assume that the emissivity does not vary with wavelength (graybody assumption) and find an exact solution to the true temperature. With an increasing number of wavelengths covered, one can apply more realistic (and complicated) models for the spectral behavior of the emissivity and find an exact solution to the true temperature. In applications where one deals with smooth, non-oxidized metallic surfaces, these approaches might be justified because the dependence of the optical properties (and hence the emissivity) on temperature and wavelength is very well understood [8]. Even then the big drawback of multiwavelength approaches is that the uncertainty of the true temperature cannot be estimated [9], and hence the quality of the temperature measurement cannot be assessed. If the surface is not expected to stay smooth (as in free surface shock physics experiments), then none of the standard multiwavelength approaches found in the literature will provide a satisfactory solution to the emissivity problem. Nevertheless, it is still preferable to use multiwavelength techniques in pyrometric shock physics experiments, since the temperature readings (assuming lower and upper bounds for the value of the normal spectral emissivity) at different wavelengths help determine if one is dealing with either background light or temperature non-uniformities (this will become clear in the next section).

1.4. Temperature Inhomogeneities

Shock physics deals with highly dynamic processes in order to achieve pressures (up to several Mbar) which are beyond the reach of any static method. Due to the methods required to achieve these extreme pressures, phenomena which lead to a non-uniform temperature distribution in the surface under investigation are important and have to be addressed. Common phenomena causing temperature inhomogeneities in free surface experiments are:

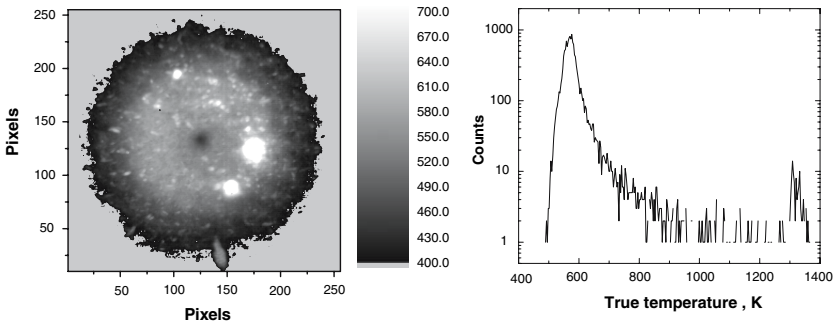

Fig. 2. IR-image of free surface Basalt at a peak pressure of 14.9 GPa (left, scale: 90 μm/pixel) and histogram of the temperature distribution at the region of pressure uniformity (right).

- Microjets due to machining grooves or random surface roughness
- Hot ejecta
- Porosity or surface voids (most common in rocks and minerals)
- Composition inhomogeneities (also in rocks and minerals)
- Shear-banding in regions where proper strain rates occur (only in metals with certain stress-strain relationships)

Figure 2 shows an infrared camera image of a free surface shock experiment on basalt. The peak pressure in this experiment is about 15 GPa; the image was taken 503 ns after breakout with a gate time of 513 ns. The center wavelength of the IR-camera is 4.16 μm with a FWHM of approximately 1.0 μ m. The distribution of the true temperature (assuming an emissivity of 0.8) is shown to the right of the IR image. The diameter of the hot region is slightly larger than 12 mm; the cold spot in the center is due to the obstruction of the image by the photon doppler velocimetry [10] probe.

1.5. Dynamic Range and Lower-Temperature Limit

An additional consideration in applying pyrometry to shock physics experiments is the temperature range that can be covered with a pyrometer for a given wavelength. Since the temperature to be determined is not *a priori* well known in shock physics experiments, this range has to be as large as possible. Figure 3 shows the relative dynamic range (maximum temperature reading before detector saturation minus minimum temperature reading based on a certain signal-to-noise ratio, over the minimum temperature reading) of a pyrometer. One can see that the dynamic range increases dramatically with increasing wavelength (almost an

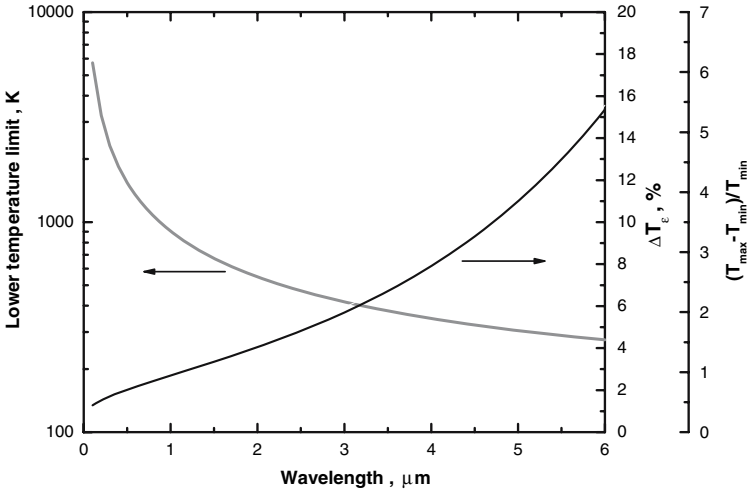

Fig. 3. Dynamic range $((T_{\max} - T_{\min})/T_{\min})$, lower temperature limit $(T_{\min})$, and relative uncertainty due to unknown emissivity of a pyrometer as a function of wavelength.

order of magnitude within the wavelength range considered here). This is a direct consequence of the decrease of the relative change of thermal radiance over the relative change of temperature over the product of wavelength and temperature (Fig. 1). For the same reason the uncertainty due to unknown emissivity increases as well from a value of 2% at 1 μm to more than 15% at 6 μm, as also seen in Fig. 3. For calculation of the relative uncertainty due to an unknown emissivity, a value of the normal spectral emissivity of 0.8 with an uncertainty of ± 0.2 over the entire wavelength range was assumed. This is a very realistic assumption for basalt; for the case of metals where the emissivity is very small at room temperature (less than 2% in the case of polished molybdenum at 5 μm), the uncertainty caused by an unknown emissivity can be much larger.

Figure 3 also shows the minimum temperature that can be detected with a pyrometer at a given wavelength. This temperature increases with decreasing wavelength, as seen from the exponential growth of the signal with increasing temperature and wavelength (Fig. 1). This curve becomes almost flat at wavelengths above 5 μm, hence almost nothing can be gained by doing pyrometry at wavelengths much greater than 5 μm. The calculations shown in Fig. 3 are based on an indium-antimonide detector with state-of-the-art electronics. The pyrometer from which the characteristics for this calculation have been taken is described in more detail in Ref. [11]. The bandwidth for this calculation has been assumed to be a tenth of the center wavelength (the reason for this assumption can be found in

Ref. [4]). For wavelengths shorter than 1.2 μm, the use of InSb detectors is not reasonable and hence this figure is not completely accurate below this wavelength limit. Nevertheless, the authors calculated the same curve based on the characteristics of a state-of-the-art photomultiplier tube and the difference with the InSb curve was sufficiently insignificant to present InSb-based data only for simplicity.

2. SIMPLE MODEL FOR TEMPERATURE NON-UNIFORMITIES

A simultaneous temperature measurement with pyrometry (single point, high time resolution) and thermography (e.g., IR-camera; spatial resolution depending on optical system, only one point in time with a rather large gate time) is almost never possible. Therefore, the pyrometer readings at different wavelengths have to be fitted with physics-based models to gain insight into the temperature distribution. The actual temperature distribution due to hot-spots in an experiment on basalt is also shown in Fig. 2 and consists of two components. The main surface temperature (more than 95% of the surface area) is at a temperature of 600 ± 57 K, while some 1.5% of the surface area is at a temperature of 1320 ± 20 K. Therefore, a simple model assuming only two temperature components with an area fraction adding up to unity might be sufficient to describe the pyrometer reading at different wavelengths. Equation (2) below gives the total radiance seen by a pyrometer due to these two components. This radiance can be described by an effective uniform surface temperature T_{eff}. The hot-spots are at a temperature T_{HS} with an area fraction α, the temperature of the remainder of the surface is at a temperature T with an area fraction (1-α). The emissivity ε is assumed not to be dependent on temperature ($\varepsilon_{\text{HS}} = \varepsilon = \varepsilon_{\text{eff}}$):

$$L = \frac{(1-\alpha)\,\varepsilon c_1}{\lambda^5\left(e^{\frac{c_2}{\lambda T}} - 1\right)} + \frac{\alpha \varepsilon c_1}{\lambda^5\left(e^{\frac{c_2}{\lambda T_{\text{HS}}}} - 1\right)} = \frac{\varepsilon c_1}{\lambda^5\left(e^{\frac{c_2}{\lambda T_{\text{eff}}}} - 1\right)} \tag{2}$$

In this equation the constant factors c_1 and ε cancels out and T_{eff} can be expressed as a function of T_{HS}, T, α, and λ. This relation is given in the following equation:

$$T_{\text{eff}} = \frac{c_2}{\lambda \ln\left(\dfrac{1}{\dfrac{(1-\alpha)}{\left(e^{\frac{c_2}{\lambda T}} - 1\right)} + \dfrac{\alpha}{\left(e^{\frac{c_2}{\lambda T_{\text{HS}}}} - 1\right)}} + 1\right)} \tag{3}$$

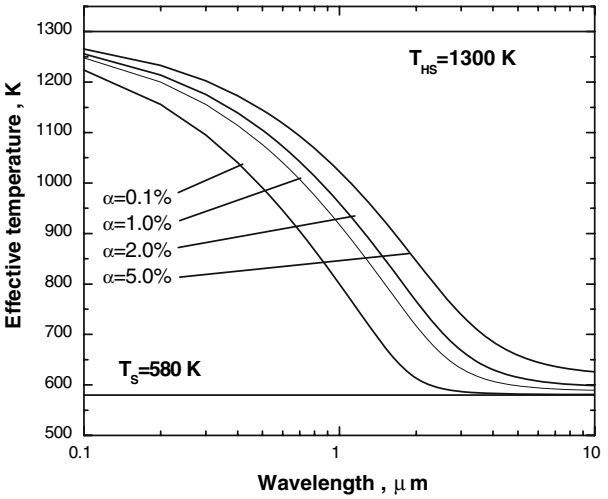

Fig. 4. Temperature as seen by a pyrometer for a surface temperature of 580 K and a hot-spot temperature of 1300 K for four different area fractions over the wavelength range of 0.1–10.0 μm.

Since it is difficult to picture the interdependence of all the contributions to the effective temperature, a graphical representation of Eq. (3) (for four different area fractions between 0.1 and 5%) is shown in Fig. 4 for a surface temperature T of 580 K and a hot-spot temperature of 1300 K (these values are the predicted free surface temperature of basalt at 15 GPa as well as the melting temperature of basalt and agree with the data shown in Fig. 2). One can see that long wavelengths are almost insensitive to hot-spots. The wavelength at which the contribution of the hot-spots becomes significant depends on the hot-spot area fraction as well as on the hot-spot temperature. Another way to represent Eq. (3) in a graphic way is shown in Fig. 5. Here the effective temperature for a surface temperature of 580 K and a fixed area fraction of 1% is given as a function of the hot-spot temperature. From this figure one can see that even a hot-spot temperature only slightly above the surface temperature is enough to alter the reading of a short-wavelength channel significantly. Long-wavelength channels are almost invulnerable to hot-spots, but if one keeps in mind that the uncertainty due to an unknown emissivity is a factor of six larger at 5 μm compared to that at 0.5 μm (see Fig. 3), then measuring the temperature at long wavelengths exclusively is not a remedy to this problem.

It is known from the literature [12] that the normal spectral emissivity in most cases increases with temperature and hence the assumption of

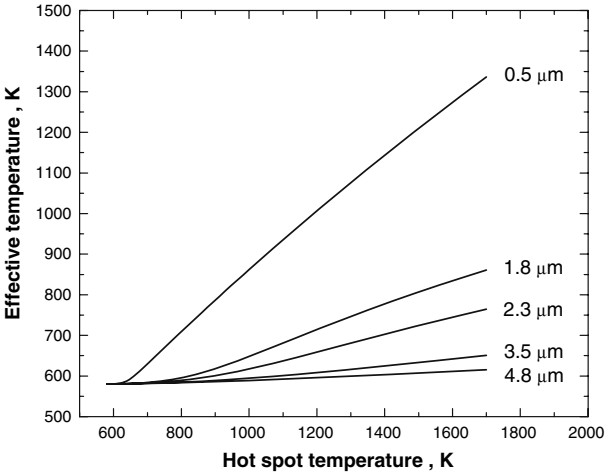

Fig. 5. Temperature as seen by at a surface temperature of 480 K and hot-spot area fraction of 1% as a function of the hot-spot temperature for different wavelengths.

a constant emissivity in order to obtain Eq. (3) is not valid. Nevertheless, the change of emissivity with temperature is very small and can be neglected compared to the exponential change of radiance with temperature.

3. RESULTS

Temperature data have been taken using a four-wavelength IR pyrometer and also by IR-imaging different experiments using the same experimental setup on tin. Neither the pressure nor the temperature distribution in this type of experiment (direct driven shocks by attaching high explosives to the back of the sample; for a more detailed description, see Ref. [6]) is very reproducible. Therefore, fitting the pyrometer data with Eq. (3) and then comparing the result to the temperature distribution measured by thermography would not be reasonable. For this reason realistic pyrometer data have been simulated using the measured temperature distribution shown in Fig. 2 (this is possible because the calibration factors for each channel of the pyrometer are well known, stable, and reproducible for the pyrometer described in Ref. [11]) and then this pyrometer data were fit using Eq. (3). Values for the surface temperature and the hot-spot temperature, as well as the area fraction, are thusly obtained. Table I gives the simulated effective temperatures as well as the uncertainties for this simulation. Figure 6 shows the fits using only the four longer wavelengths (top) and all five wavelengths (bottom). The black curve shows the fit through

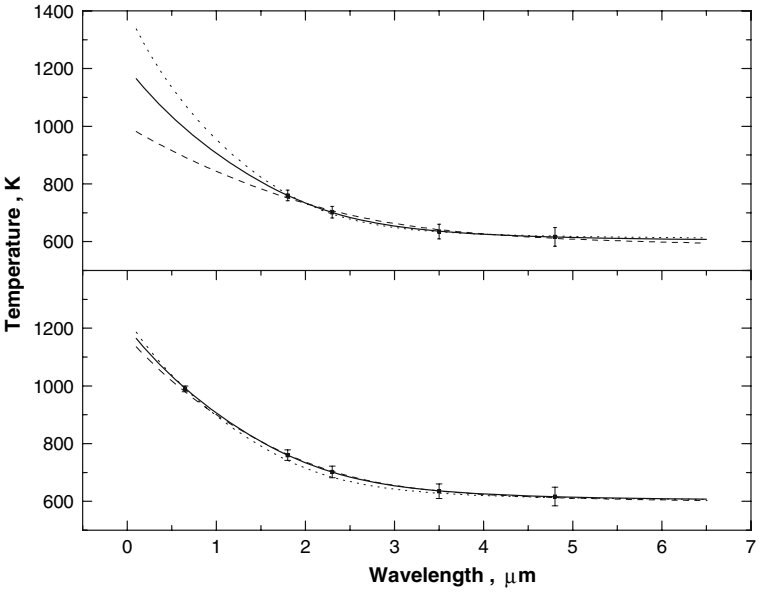

Fig. 6. Fits to pyrometry data by Eq. (3).

the data points whereas the dotted and dashed curves show the fit with the maximum and minimum hot-spot temperatures that can be obtained by having the fitted curve within the error bars. The results of these fits are given in Table II. From this, it becomes obvious that even though short wavelengths are also very vulnerable to hot-spots, they are nevertheless still very important in constraining the hot-spot temperature. Even when using all five wavelengths for the analysis, the area fraction is still not constrained very well.

The obtained results for the surface temperature are in very good agreement even when using only four wavelengths. In order to obtain a reasonable reading for the hot-spot temperature, one needs to obtain a temperature measurement at a wavelength as short as possible. The measurement spot of the pyrometer has to be large enough (compared to the spatial structure of the temperature distribution) in order to get a reasonable reading of the temperature distribution of the surface. If the measurement spot size is very small, one might only sample either a hot-spot or the temperature of the surface where no hot-spots occur. In this case the reading of different wavelength channels will give a consistent reading although the absolute value of this reading could be highly inaccurate.

Table I. Simulated Effective Temperature (T_{eff}) for Five Wavelengths λ Obtained from the Temperature Distribution shown in Fig. 2 and Characteristics for a Four-Wavelength Pyrometer Described in Ref. [11]

λ (μm)	T_{eff} (K)	ΔT_{eff} (K)
0.65	990	10
1.80	760	18
2.30	702	20
3.50	635	25
4.80	616.5	32.5

The temperature uncertainties ΔT_{eff} are calculated assuming lower and upper bounds of the emissivity of 0.6 and 1.0.

Table II. Results of Fitting the Data Shown in Table I by Eq. (3)

λ (μm)	T (K)	ΔT (K)	T_{HS} (K)	ΔT_{HS} (K)	α	$\Delta\alpha$
0.65–4.80	580	30	1256	26	0.021	0.008
1.80–4.80	585	40	1247	214	0.018	0.009

4. CONCLUSIONS

When pyrometry is applied to shock physics experiments, one has to take into account the dynamics of the experiment. For example, background shock light due to nitrogen luminescence, high-explosive burn products, or laser light can invalidate the results of such an experiment. Engineering approaches have to be applied in order to mitigate these problems. Non-uniformities in the surface temperature are also a common problem in shock physics. These cannot be avoided in most cases even if the experiment is designed properly. In the more common case when the non-uniformity is in the plane of the surface, then a two-temperature approach can be very useful in extracting the surface temperature, the hot-spot temperature, and to a certain degree the area fraction of the hot-spots. Meaningful information can best be extracted with a wavelength range as broad as possible and all channels giving a temperature reading. A temperature reading at all wavelengths covered can be achieved by using neutral density filters in the optical path of the longer wavelengths in order to raise the temperature range covered to higher temperatures. In many cases the post-shock temperatures are very low and challenge the lower-temperature threshold of the instrument. Raising the temperature range by using neutral density filters in these cases is not an option.

For the case when the temperature non-uniformity is due to thermal radiation from a hot anvil, the situation becomes more complicated, since then the temperature of the anvil as well as the optical properties must be known as a function of temperature and pressure. Fitting these data requires even more wavelength channels, and anyway the fitting process might not put many constraints on these properties. The authors are presently addressing this problem. Physically reasonable values for the optical properties of the anvil are being generated. Also physics-based models are being applied to results obtained some years ago on shock-loaded molybdenum [6] in order to extract meaningful temperature data from these experiments.

Applying multiwavelength approaches as described in the pyrometry literature is problematic in well-behaved or static experiments, where no surface roughness and uniform temperatures are involved. Applying these pyrometric approaches to shock physics experiments is not recommended. Nevertheless, using more than one wavelength is very important because, if the measurement spot on the surface is sufficiently large, this technique shows up any problems.

Single-wavelength pyrometry applied to shock physics experiments requires additional knowledge of the temperature uniformity of the experiment as well as confidence that none of the other problems described in this paper are present. Using only one wavelength can be very deceiving and is also not recommended.

ACKNOWLEDGMENTS

The work was performed under the auspices of the US Department of Energy under Contracts W-7405-ENG-36 and DE-AC52-06NA25396.

REFERENCES

1. A. Seifter, K. Boboridis, and A. W. Obst, *Int. J. Thermophys*. **25**:547 (2004).
2. Y. H. Zhou and Z. M. Zhang, *J. Heat Transfer* **125**:462 (2003).
3. "Standard Test Method for Noise Equivalent Temperature Difference of Thermal Imaging Systems," *ASTM Standard E 154313-94* (1994).
4. D. P. DeWitt and G. D. Nutter, *Theory and Practice of Radiation Thermometry* (John Wiley & Sons, New York, 1988).
5. S. A. Raikes and T. J. Ahrens, *Geophys. J. R. Astron. Soc*. **58**:717 (1979).
6. A. Seifter, M. Grover, D. B. Holtkamp, J. R. Payton, P. Rodriguez, W. D. Turley, and A.W. Obst, *"High Speed Photography and Photonics," SPIE Paper #5580-125*, Virginia (2005), pp. 18–23.

7. G. Neuer and L. Fissler, "Crytical Analysis of the Different Methods of Multiwavelength Pyrometry," in *Temperature: Its Measurement and Control in Science and Industry*, Vol. 6, J. F. Schooley, ed. (AIP, New York, 1992), p. 797.
8. M. Born and R. Wolf, *Principles of Optics*, 7th Ed. (Cambridge University Press, 1999).
9. K. Boboridis, A. Seifter, A. W. Obst, and D. Basak, *Int. J. Thermophys.* **25**:1187 (2004).
10. O.T. Strand, D.R. Goosman, C. Martinez, T.L. Whitworth, and W.W. Khylow, *Rev. Sci. Instr.* **77**:083108 (2006).
11. K. Boboridis and A. W. Obst, "A High-Speed Four-Channel Infrared Pyrometer," in *Temperature: Its Measurement and Control in Science and Industry*, Vol. 7, Part 2, D. C. Ripple, ed. (AIP, New York, 2003), p. 759.
12. A. Seifter, F. Sachsenhofer, and G. Pottlacher, *Int. J. Thermophys.* **23**:1267 (2002).